BIOCHEMISTRY
including biophysical chemistry & molecular biology

Article

pubs.acs.org/biochemistry

Multiple Drug Transport Pathways through Human P-Glycoprotein

James W. McCormick, Pia D. Vogel, and John G. Wise*

Center for Drug Discovery, Design and Delivery, Center for Scientific Computing, and Department of Biological Sciences, Southern Methodist University, Dallas, Texas 75275-0376, United States

Supporting Information

ABSTRACT: P-Glycoprotein (P-gp) is a plasma membrane efflux pump that is commonly associated with therapy resistances in cancers and infectious diseases. P-gp can lower the intracellular concentrations of many drugs to subtherapeutic levels by translocating them out of the cell. Because of the broad range of substrates transported by P-gp, overexpression of P-gp causes multidrug resistance. We reported previously on dynamic transitions of P-gp as it moved through conformations based on crystal structures of homologous ABCB1 proteins using *in silico* targeted molecular dynamics techniques. We expanded these studies here by docking transport substrates to drug binding sites of P-gp in conformations open to the cytoplasm, followed by cycling the pump through conformations that opened to the extracellular space. We observed reproducible transport of two substrates, daunorubicin and verapamil, by an average of 11−12 Å through the plane of the membrane as P-gp progressed through a catalytic cycle. Methylpyrophosphate, a ligand that should not be transported by P-gp, did not show this movement through P-gp. Drug binding to either of two subsites on P-gp appeared to determine the initial pathway used for drug movement through the membrane. The specific side-chain interactions with drugs within each pathway seemed to be, at least in part, stochastic. The docking and transport properties of a P-gp inhibitor, tariquidar, were also studied. A mechanism of inhibition by tariquidar that involves stabilization of an outward open conformation with tariquidar bound in intracellular loops or at the drug binding domain of P-gp is presented.

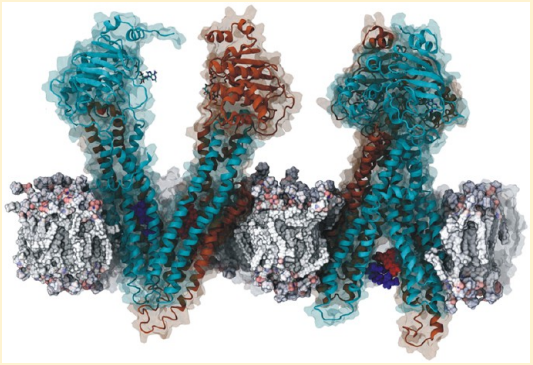

The mammalian ATP binding cassette transporter, P-glycoprotein (P-gp), is present in many tissues[1] and helps in detoxifying cells by pumping xenobiotics across the plasma membrane.[2] P-gp is able to bind and transport a diverse range of cationic amphipathic molecules ranging in size from 100 to 4000 Da.[3] This broad transport substrate spectrum is used to remove cytotoxic compounds from cells of the intestinal epithelium, adrenal glands, placenta, the brush border of the renal tubule, the canalicular membrane of hepatocytes, pancreatic ductile cells, and capillary endothelial cells of the brain and testes.[4,5] Because of this broad range of substrates, P-gp is associated with multidrug resistance (MDR) in the chemotherapies of many types of cancers,[6−8] has been implicated in Alzheimer's disease,[9,10] and has proven to be problematic in the management of HIV/AIDS.[11] P-gp is an ∼170 kDa protein consisting of two pseudosymmetrical halves, each containing a nucleotide binding domain (NBD) and a transmembrane domain (TMD).[12] It has been hypothesized that ABC-transporter proteins undergo large conformational changes powered by the binding and hydrolysis of ATP and that these changes alter the transmembrane domains from "open to the cytoplasm" (inward-facing) to "open to the extracellular space" (outward-facing) conformations (see, for example, refs 13−21). These conformational changes are thought to allow the movement of substrates across the membrane from the cytoplasmic to the extracellular phospholipid leaflets,[19,22] ultimately resulting in the dissociation of the substrates from the extracellular membrane leaflet into the extracellular space. It is not clear whether such active transport involves driving the substance toward the external space or whether the rearrangement of transmembrane helices simply alters access from the cytoplasmic to the extracellular space. In either case, the removal of cytotoxins by P-gp from the cytoplasm of cells has been suggested to be an important molecular mechanism of multidrug resistance.[23,24] The inward-facing structures of P-gp from mouse,[25,26] *Caenorhabditis elegans*,[27] and some bacterial homologues[19] have fully disengaged NBDs with the transmembrane drug binding domains (DBDs) open to the inside of the cell. These open inside conformations of P-gp have been demonstrated to be remarkably flexible.[28] The highest-resolution X-ray structural models of ABCB1 transporters were obtained from a multidrug resistance pump from the bacterium *Staphylococcus aureus*,[22,29] a prokaryotic homologue that shares some drug transport substrates, pumping activities, and inhibitors with P-gp.[30] The *S. aureus* structures exhibit fully engaged NBDs with nucleotides bound and DBDs that are open to the outside.[22,29] We previously reported the simulation of conformational

Received: January 8, 2015
Revised: June 26, 2015
Published: June 30, 2015

ACS Publications © 2015 American Chemical Society

DOI: 10.1021/acs.biochem.5b00018
Biochemistry 2015, 54, 4374−4390

changes in models of human P-gp as the transporter undergoes a transition though a putative catalytic cycle.[31] We used targeted molecular dynamics techniques[32−35] and structures of human P-gp homologues that had drug binding domains positioned "wide open" to the cytoplasm (mouse 3G60 structure,[36] no nucleotides bound), "partially open" to the cytoplasm (*Vibrio cholerae* 3B5X structure,[19] no nucleotides bound), "open" to the extracellular space (*S. aureus* SAV1866 2HYD structure, ADP bound to the nucleotide binding sites[22]), and "wide open" to the extracellular space (*Salmonella typhimurium* MsbA structure 3B5Z with an ADP-vanadate transition-state analogue bound at the nucleotide binding site[19]) to simulate the conformational transitions of P-gp during a putative catalytic cycle.[31] These dynamic models of P-gp proved to be useful in the identification of several novel inhibitors of the transporter that target its nucleotide binding domains.[37] In more recent work from our lab using these targeted molecular dynamics techniques, corrected versions of the mouse structures as reported in refs 25 and 26 and new structures of eukaryotic P-gp from *C. elegans*[27] have been employed. In a recent report[38] using TMD techniques that were similar to those reported previously by us,[31] drug transport simulations were attempted. These simulations, however, did not show significant movement of transport substrates through P-gp.[38]

In the work reported here, an in-depth look at the movement of two transport substrates through P-gp from one side of the membrane to the other was investigated during targeted molecular dynamics simulations of putative transport cycles as developed previously.[31] We used the chemotherapeutic daunorubicin, a known transport substrate of P-gp, and the antihypertensive agent verapamil, a known modulator of P-gp-conferred multidrug resistances of cancers,[39−41] in these simulations. The simulation experiments were replicated six times each. We observed large transport substrate movements from cytoplasmic to extracellular positions in all of the simulations in which daunorubicin and verapamil were used. To simulate the conformational changes of P-gp during a catalytic cycle, forces were applied to selected Cα atoms of the protein to induce the targeted changes in the P-gp structures. No forces were directed at the transport ligands other than those applied by the moving protein. The conformational changes were chosen so P-gp would force the drug binding sites to undergo transitions from wide open to the cytoplasm to wide open to the extracellular space. These studies have allowed the investigation of protein-driven movement of transport substrates through the membrane. In additional experiments, we also examined the behavior of a potent inhibitor of P-gp, tariquidar.[42]

The simulations presented here show that transport substrates docked into different initial binding sites within the cytoplasmic leaflet of the drug binding domains of P-gp were transported through the membrane as P-gp underwent a transition from inside open to outside open conformations. Repeated simulations with these transport substrates revealed associations with different parts of the membrane-embedded transmembrane helices of P-gp. The results suggest that once bound, movement of substrates through P-gp occurs through at least two general pathways via stochastic mechanisms.

MATERIALS AND METHODS

Materials. The Visual Molecular Dynamics program suite (VMD)[43] was extensively used in this work. Molecular dynamics experiments were performed with NAMD version 2.9[44] using the CHARMM27 force field.[45] AutoDock 4.2[46] was used for initial docking of transport ligands to the drug binding domains of P-gp. Computational resources of the SMU Center for Scientific Computation were used.

Ligand Docking to P-gp. Prior to the start of molecular dynamics simulations, AutoDock 4.2[46] or AutoDock Vina[47] was used to dock daunorubicin or verapamil using a human P-gp structure equivalent to the mouse 4KSB crystal structure[25] as described previously.[31] Ligand interactions were limited to the cytoplasmic extensions of the transmembrane helices and transmembrane sections of P-gp. Binding of ligand to NBDs was not investigated. For AutoDock 4.2 experiments, grids were calculated using 0.375 Å spacing in a 126 $Å^3$ cube. For each ligand, 100 genetic algorithm experiments were performed using 3000000 energy evaluations, a population size of 300, and 27000 generations. The ligand docking positions resulting from these experiments were ranked by predicted affinities. The conformational pose of the ligand that was predicted to have the highest affinity was used as a starting point in the molecular dynamics simulations, except where indicated in the text. For AutoDock Vina experiments, 300 replicates (exhaustiveness of 300) were performed using a cube having lengths of 56 Å per side, unless otherwise noted.

Molecular Dynamics Simulations. Daunorubicin and verapamil were parametrized as previously described by us for other nonstandard molecules.[48] Equilibrium geometries were obtained from *ab initio* quantum mechanical simulations using GAMESS and an unrestricted Hartree−Fock 6-31 basis set.[49] Parameter and topology files were created using these data and as described in ref 50. We also used the *antechamber* module[51] from the *AMBER14* suite of programs[52] together with the *general AMBER force field*[53] and the AM1-BCC charge estimation methods[54,55] to parametrize daunorubicin, verapamil, and tariquidar. To test the influence of the parametrization methods used on the results of the simulations, results using the AMBER-produced parameters for molecular dynamics simulations of verapamil were compared to those produced by the methods of Fajer and co-workers[50] in experiments that were otherwise identical to those shown in Figure 3A (see below). No significant difference in the behavior of the verapamil parametrized using the AMBER General Force Field for organic molecules (version 1.7, November 2013) compared to verapamil parametrized with GAMESS as described in ref 50 was observed (data not shown).

Models for human P-glycoprotein inserted into a POPC phospholipid bilayer, and including nucleotides, Mg^{2+} ions, Na^+ and Cl^- counterions, and water, were created as described previously.[31] Molecular dynamics (MD) simulations were performed with constant temperature and pressure (*NPT* ensemble) in a periodic cell using Langevin temperature and pressure control, as well as particle-mesh Ewald electrostatics calculations at 310 K. Targeted molecular dynamics (TMD) simulations[56,57] on P-gp were performed using target coordinates derived from mouse Pgp[25] [Protein Data Bank (PDB) entry 4KSB)] the Sav1866 transporter (PDB entry 2HYD),[22] and MsbA structures 3B5X and 3B5Z[19] as previously described.[31] Briefly, the target structures were aligned using STAMP[58] as implemented in the Multiple Alignment[59] module of VMD,[43] and the coordinates of homologous Cα atoms for each structure were used as target coordinates of the respective Cα atoms of the human P-gp model. TMD was performed with each target in sequential simulations. Forces were applied using

DOI: 10.1021/acs.biochem.5b00018
Biochemistry 2015, 54, 4374−4390

tcl scripts in NAMD to the selected Cα atoms of the human P-gp model to gently move the atoms toward the respective target coordinates. The magnitudes of these forces were calculated to be inversely proportional to the rmsd of the distances separating the selected Cα atoms and the target coordinates. The final systems used in TMD simulations shown in Figure 1

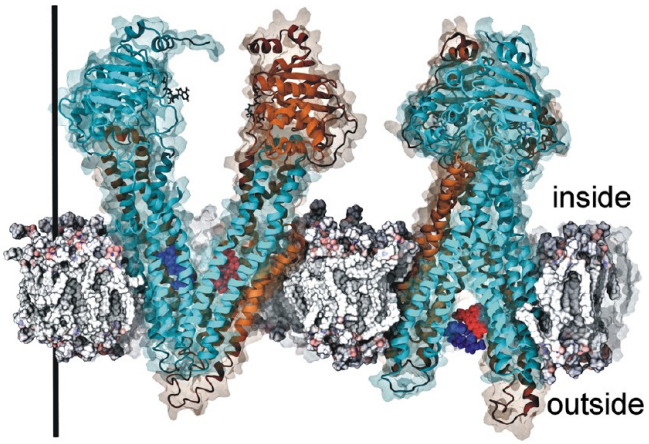

Figure 1. Human P-glycoprotein conformations extracted at the start and end of targeted molecular dynamics simulations. Human P-gp model structures are shown at the beginning of the targeted molecular dynamics simulations (left) and at the end of the TMD simulations (right). The right-hand structure shows the protein rotated about the *Y*-axis by 90° to better visualize the opening of the transmembrane helices to the outside. Human P-gp was pushed to each structure in TMD simulations as described in ref 31 and Materials and Methods. The structures shown have calculated rmsd values for targeted Cα atoms of human P-gp to target structures of <0.3 Å. The target structure at the beginning of the simulations was mouse P-gp (4KSB),[25] and the ending target structure was the transition-state MsbA structure (3B5Z).[19] The beginning structure (left) has the drug binding sites wide open to the cytoplasm (top of the membrane) and disengaged nucleotide binding domains. The ending structure has fully engaged nucleotide binding domains with the drug binding domain wide open to the extracellular space (below the membrane). Verapamil (blue space filling representations) and daunorubicin (red space filling representations) are shown at their highest-affinity binding sites in the starting structure and what may be the release sites in the ending structure. Starting positions for the transport substrates were determined by docking experiments (Materials and Methods). The N-terminal half of the protein is shown in both ribbon and surface representations (blue), while the C-terminal half of the transporter is colored gold. The black bar shows the direction of the *Z*-axis of the system and measures approximately 150 Å.

contained 157540 atoms for P-gp with bound verapamil and 157518 atoms for the system with daunorubicin bound to P-gp. In control experiments, a ligand that should not be transported by P-gp, the methyl ester of pyrophosphate ($CH_3O_7P_2$), was added to P-gp in the same location where verapamil had docked in experiments as described above. The methylpyrophosphate system had 157482 total atoms. Experiments with tariquidar had a similar number of atoms. Each ligand-bound system was minimized, heated, and equilibrated for 2 ns before the targeted molecular dynamics scripts were initiated.

Analyses of the overall movement of verapamil, daunorubicin, methylpyrophosphate, or tariquidar during each simulation were made by calculating the centers of mass of the ligands over the course of the simulations using *tcl* programming scripts in VMD. Analyses of the interactions of individual transmembrane helices with each of the transport substrates and the negative control over the course of several simulations were also accomplished with the help of *tcl* scripts and VMD. Briefly, at equal intervals throughout a complete simulation, the numbers of contacts between the substrate and protein were determined for each transmembrane helix as well as any contacts outside of the transmembrane regions. The results were summed for each simulation frame analyzed and plotted in three-dimensional plots for each helix versus values of the progress of the simulation. Data for determining whether these interactions between transport substrate and protein were mediated by nonpolar, aromatic, polar, acidic, or basic amino acids were also collected. Results are reported either for individual simulations or the averages of all contacts for each drug at equivalent stages of simulation.

RESULTS

Molecular Simulations of the Conformational Changes in Human P-Glycoprotein during a Transport Cycle. This work builds on our previous work that aimed to understand the catalytic transitions that P-gp undergoes during a putative transport cycle. To simulate the actual molecular transport, we added transport substrates into the drug binding domain (DBD) of P-gp by ligand docking methods and then simulated the transport cycle using targeted molecular dynamics (TMD) simulation techniques. We reasoned that if the putative catalytic transitions presented previously[31] were relevant approximations of the normally occurring P-gp-catalyzed drug transport, then freely mobile, completely unrestrained ligands known to be transport substrates of P-gp should move from the cytoplasmic side of the membrane to the extracellular side of the membrane during the course of the simulations. Minimally, if the conformational changes shown previously[31] were relevant to P-gp drug transport, the ligands should at the very least gain access to the extracellular membrane leaflet.

To detect possible effects on ligands bound to the drug binding sites of P-gp, we first performed TMD experiments with either daunorubicin or verapamil bound to the transporter. These ligands are known to be transported by P-gp.[60,61] Daunorubicin or verapamil was docked in separate experiments to models of human P-gp in the starting conformation (with drug binding domains wide open to the cytoplasmic side of the membrane, corresponding to the mouse 4KSB structure). Figure 1 (left panel) shows a composite figure of the two transport ligands on a single protein (verapamil colored blue and daunorubicin red). It is interesting that the predicted highest-affinity docking poses for daunorubicin and verapamil had the substrates bound to opposite sides of this open to the cytoplasm conformation of P-gp.

Figure 2 shows a close-up of the initial starting positions of daunorubicin (left) and verapamil (right) in the two drug binding subsites of P-glycoprotein that are equivalent to the poses shown in the composite depiction of Figure 1 (left). While the predictive ability of docking tools is limited, especially for large search areas, docking was used as a way to generate a plausible starting point for molecular dynamics simulations. After docking and assembly of a complete system, including P-gp, lipids, water, and ions, the docking poses for each ligand were allowed to relax in molecular dynamics simulations after being brought to 310 K. This relaxation of the docking poses varied the starting positions of verapamil and daunorubicin before the targeted molecular dynamics simu-

DOI: 10.1021/acs.biochem.5b00018
Biochemistry 2015, 54, 4374−4390

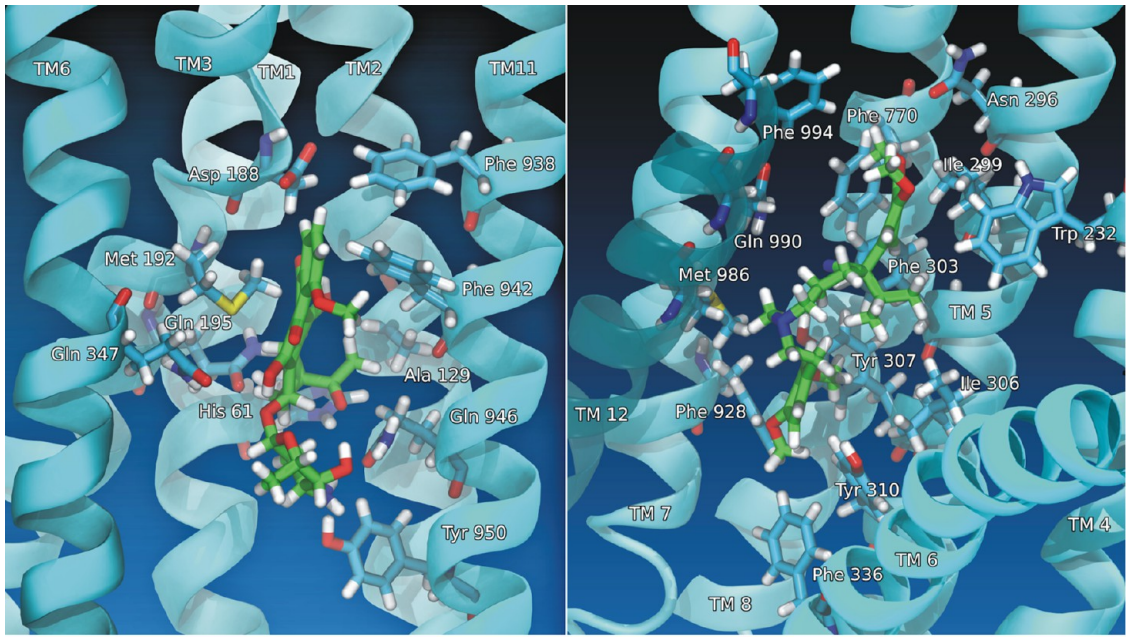

Figure 2. Structures of human P-glycoprotein with daunorubicin and verapamil bound. P-gp is colored cyan with the labeled α-helices drawn in cartoon representation. The amino acid side chains within 3 Å of daunorubicin (left) and verapamil (right) are drawn as sticks and are labeled. Daunorubicin and verapamil are shown as green sticks. Linear depth cueing is implemented in these figures.

lations were initiated (see below). Quantification of the resultant variation in initial ligand positions before the start of targeted molecular dynamics simulations for the six independent equilibrations per ligand showed rmsd values relative to the initial docking position of 3.2 ± 0.4 Å with a range of 2.6−3.8 Å for daunorubicin and 4.9 ± 1.0 Å with a range of 3.9−6.7 Å for verapamil. Figure 2 shows unique interactions of each drug in its different subsite on P-gp. While daunorubicin interacted with transmembrane helices (TMs) 1−3, 6, and 11, verapamil predominantly interacted with TMs 4−8 and 12. Table 1 of the Supporting Information identifies the amino acid residues and the corresponding transmembrane helices that were found to be within 4.5 Å of the highest-affinity docking poses of verapamil and daunorubicin in this initial conformation of the transporter after the docked ligands were allowed to relax in the equilibration phase of the MD simulations. Table 1 of the Supporting Information also points out residues that have been experimentally identified[26,62−69] or computationally identified[70] to be part of the drug binding sites of P-gp. Each drug binding subsite had a variety of interactions with different types of amino acid residues, but as expected, nonpolar and aromatic interactions dominated both the daunorubicin and the verapamil binding sites. Also of interest in Figure 2 are the polar interactions of P-gp with the polar portions of daunorubicin. Verapamil has a computed octanol/water partition coefficient (xlogP3) of 3.8 and is much less polar than daunorubicin (xlogP3 of 1.8; both values were obtained from the NCBI PubChem database). It therefore seems reasonable that verapamil interacted mainly with nonpolar and aromatic residues of P-gp with only an occasional polar contact, while daunorubicin displayed more frequent interactions with polar and even charged residues (Table 1 of the Supporting Information). Daunorubicin was observed in a few instances to contact residues outside of the TM region of P-gp (residues 875−879) during molecular dynamics, but it should be noted that all of these contacts were less than approximately one helical turn toward the cytosolic side of TM10. The initial docking modes for both daunorubicin and verapamil seemed to be reasonable starting points for the TMD simulations.

Movement of Daunorubicin and Verapamil through P-Glycoprotein. During the targeted molecular dynamics simulations presented here, small forces were applied to a set of selected Cα atoms of P-gp as described in ref 31and Materials and Methods. The applied forces were recalculated during each step of the simulations to direct protein movements toward the respective target Cα coordinates. These TMD techniques allowed us to continuously simulate the movement of P-gp domains starting from conformations that had the DBD wide open to the cytoplasm (4KSB) to conformations with the DBD slightly opened to the cytoplasm and NBDs partially engaged (3B5X target), to those with fully engaged NBDs and DBD opened to the exterior (2HYD target), and to a final conformation with NBDs in an ATP hydrolysis transition state where the DBDs are fully opened to the extracellular space (3B5Z target). All conformational transitions were calculated in an explicit, fully hydrated system that contained a combined aqueous and membrane environment. Figure 1 shows a composite structure of P-gp with both daunorubicin and verapamil at the starting conformations (left panel) and ending conformations (right panel) from two independent simulations. Figure 1 of the Supporting Information shows snapshots of human P-gp in conformations that have Cα atoms within 0.25 Å rmsd of the four respective targets. Figures 2 and 3 of the Supporting Information show video representations of the simulated trajectories of two of the simulations reported here for daunorubicin and verapamil, respectively.

When TMD simulations were performed starting with daunorubicin bound at the drug binding domain of P-gp in the wide open to the cytoplasm conformation (as shown in Figure 1, left, and Figure 2), vectorial movement of the bound ligand perpendicular through the plane of the membrane in the direction of the extracellular space was observed in each simulation. Figure 3A (■) shows the average positions of the

DOI: 10.1021/acs.biochem.5b00018
Biochemistry 2015, 54, 4374−4390

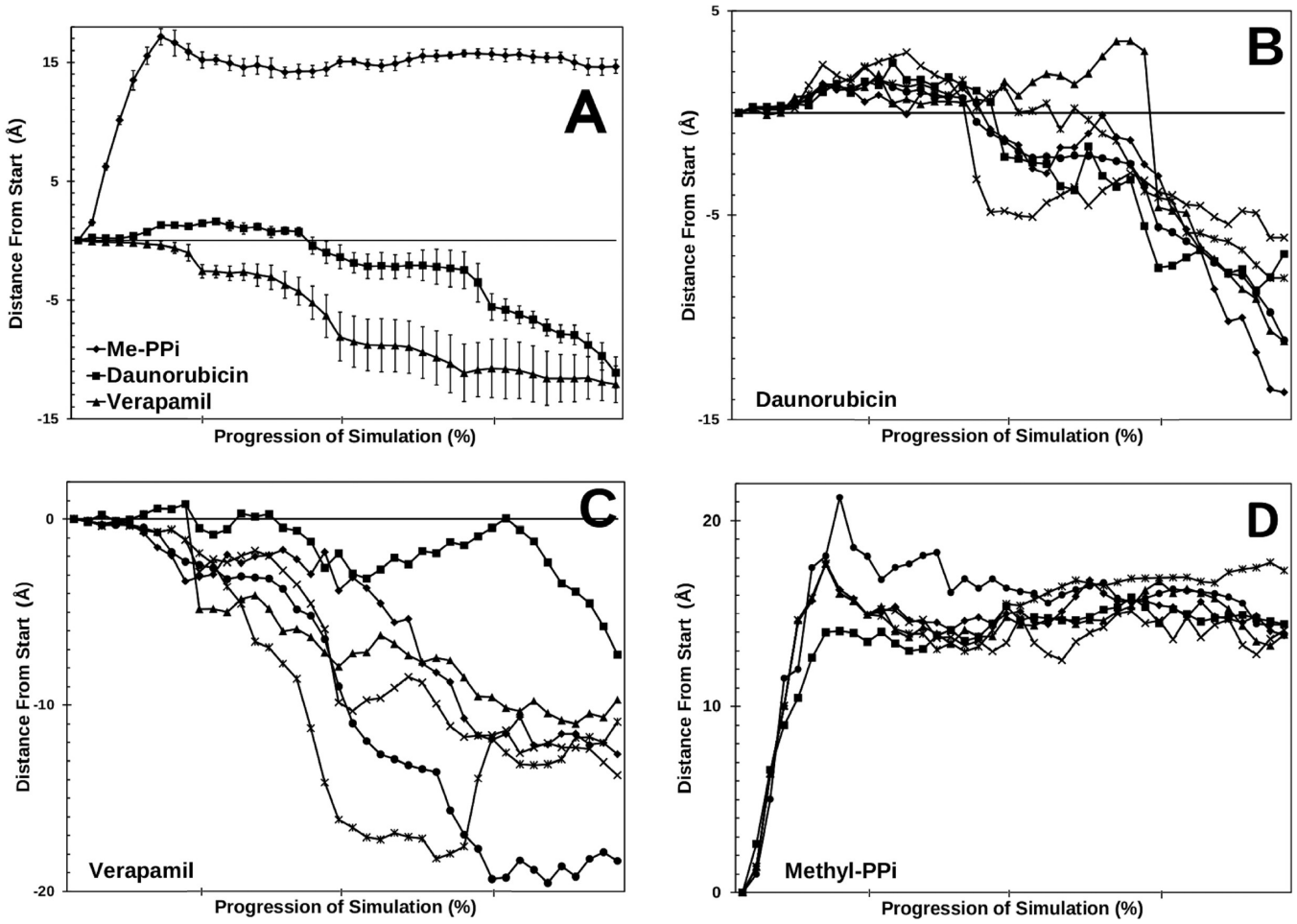

Figure 3. Movement of daunorubicin and verapamil though P-glycoprotein. (A) The center of mass of daunorubicin, verapamil, or methylpyrophosphate was calculated for each step of the simulation relative to the distance from their respective starting locations. The first quarter of the graphs represents unconstrained molecular dynamics before the application of the targeted forces. The remaining data represent the movements between targeted structures achieved by TMD techniques. The structures were oriented with the plane of the membrane in the *X*- and *Y*-directions, so that movement through the membrane is oriented on the *Z*-axis. Movement toward the extracellular space is represented by negative directions on the *Z*-axes, while movement toward the cytoplasm is represented by positive *Z*-axis directions. Distances are presented in angstroms and show the movement of the centers of mass of the ligands on the *Z*-axis. Six simulations each were performed for daunorubicin (squares), verapamil (triangles), or methylpyrophosphate (circles). The average movements of the centers of mass of each ligand are presented. Error bars represent one standard error of the mean. Movement through the membrane toward the extracellular space is equivalent to movement from positive values to negative values in these plots. (B) Same as panel A except that results for the six individual daunorubicin simulations are presented. (C) Same as panel B except that individual results for verapamil are shown. (D) Same as panel B except that individual results for methylpyrophosphate are shown.

calculated center of mass of daunorubicin that were plotted over the progress of six independent simulation experiments. The error bars represent the standard error of the mean between each of the simulations. In these experiments, the P-glycoprotein−membrane bilayer system was oriented such that the plane of the membrane was in the *X*−*Y* coordinate plane. The movement of ligand from one side of the membrane to the other could therefore be indicated as a vectorial movement on the *Z*-axes of the systems. As a reference, the black bar in Figure 1 shows the direction of the *Z*-axis relative to the membrane and transporter. In each simulation of daunorubicin bound to P-gp, a vectorial movement of the drug along the *Z*-axes from the inside surface of the membrane to the outside surface of the membrane was observed (Figure 3A,B). In these experiments, daunorubicin moved an average of approximately 11 Å from the cytoplasmic side to the external side of P-gp. Interestingly, variations in both the timing and the extent of vectorial movement of daunorubicin along the *Z*-axes were observed during the six simulations (Figure 3B, comparing each individual simulation of daunorubicin transport). This variation in vectorial transport is reflected in the standard errors of the mean shown in Figure 3A. Figure 1 (right panel) presents a composite image of human P-gp at the end of the targeted molecular dynamics simulations performed here.

Similar to the experiments shown for daunorubicin, targeted molecular dynamics simulations of verapamil docked to the drug binding sites in an open to the cytosol conformation of P-gp showed significant movement of the ligand from the cytoplasmic side of the membrane to the external side of the membrane. Figure 3A (▲) presents the average position of the center of mass of verapamil that was obtained from six independent simulation experiments. Results from each individual simulation for verapamil are shown in Figure 3C. Again, as for daunorubicin, no external forces were applied to

DOI: 10.1021/acs.biochem.5b00018
Biochemistry 2015, 54, 4374−4390

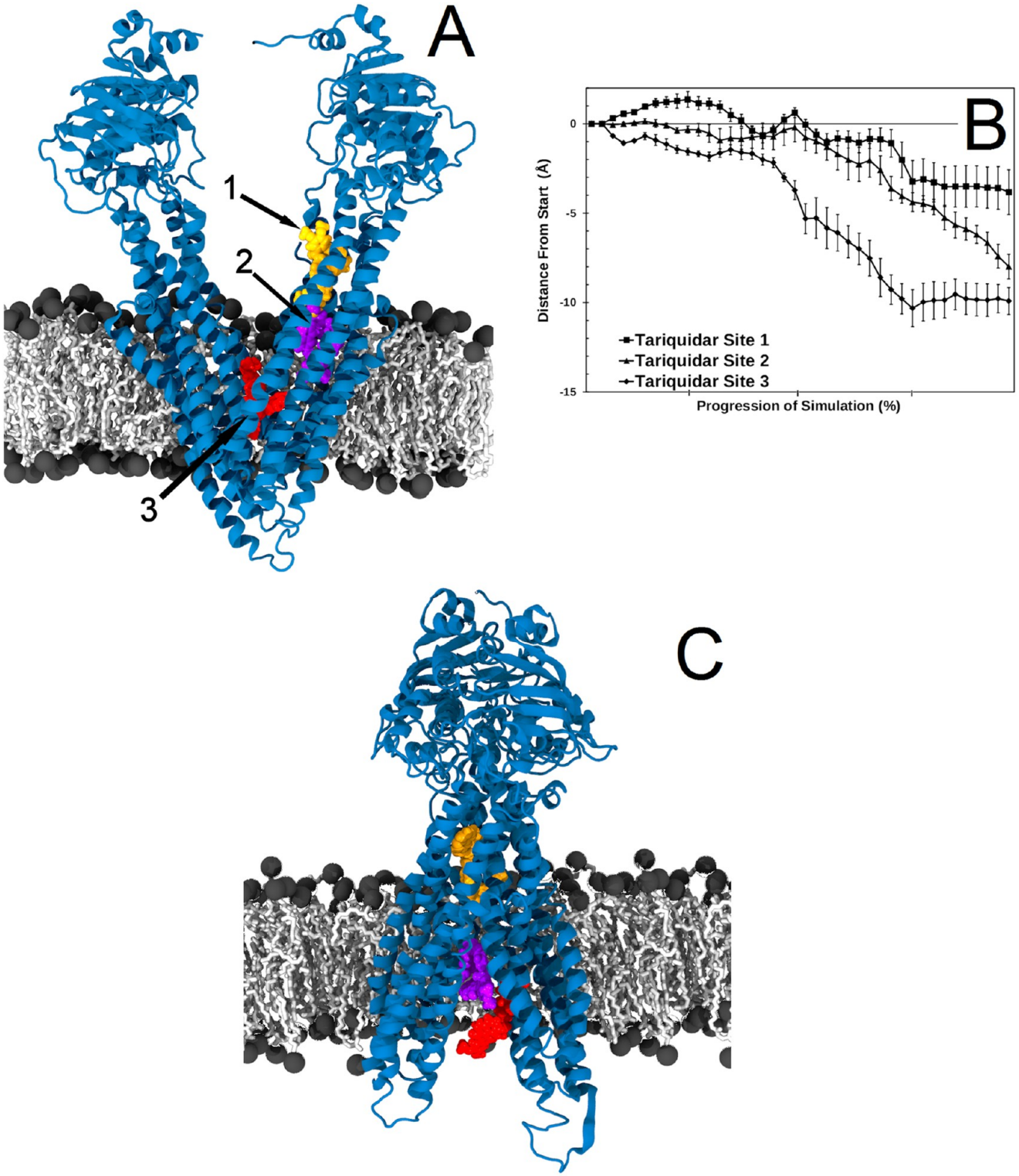

Figure 4. Movement of tariquidar when bound to P-glycoprotein. Tariquidar was docked to P-glycoprotein as described in Materials and Methods and Results and was found to preferentially bind to three different sites within P-gp. Panel A shows the three tariquidar docking sites in van der Waals spheres with site 1 colored yellow, site 2 purple, and site 3 red. Targeted molecular dynamics simulations were performed with tariquidar bound at each of these sites (sites 1−3, with six replicate simulations for each site), and the average movement of the center of mass of tariquidar is shown in panel B. Movement was calculated as described in the legend of Figure 3. Error bars represent one standard error of the mean. Panel C shows the positions of tariquidar at the end of representative simulations with the same color coding as in panel A.

the transport substrate in these simulations, yet a net vectorial movement of verapamil through the plane of the membrane averaging ∼12 Å was observed. As described for the daunorubicin simulations, variations in the extent and timing of the movements of verapamil were observed (Figure 3C), which was reflected in the errors of the mean as shown in Figure 3A. The variations in the movement of verapamil observed in these simulations were greater than those observed

DOI: 10.1021/acs.biochem.5b00018
Biochemistry 2015, 54, 4374−4390

for daunorubicin. It should be noted, however, that verapamil is a much more flexible ligand than is the rather rigid four-ring system of the anthracycline, daunorubicin. This increased flexibility of verapamil may have led to a wider variation in its measured center of mass as compared to that of daunorubicin.

Despite the variations observed in the timing and to some degree the extent of movement of the drugs through P-gp, each simulation resulted in a net vectorial transport of either daunorubicin or verapamil through the plane of the membrane (compare the left and right panels of Figure 1). The centers of mass of daunorubicin in these simulations were observed to move between 6 and 14 Å toward the external space, while the centers of mass of verapamil were observed to move between 8 Å and nearly 20 Å toward the outside (Figure 3B,C).

It was also of interest to us to determine whether transport of daunorubicin would occur when the substrate was bound in a nonoptimal docking position. To this aim, we chose a less preferred docking position for daunorubicin that was in the preferred verapamil docking site. The starting position of daunorubicin in these simulations was one of the top nine poses found in our docking experiments. The ligand in these simulations was not observed to strongly associate with any one residue and did not move toward its preferred docking position. The results of six TMD simulations performed with daunorubicin at the preferred verapamil docking site showed that daunorubicin moved an average of 13 Å through P-gp (Figure 4 of the Supporting Information).

Placing verapamil at the preferred daunorubicin docking site was more problematic, because verapamil was not found in any of the best nine docking poses in this position. We therefore performed new docking experiments with a restricted target box at the preferred daunorubicin docking site to restrict verapamil to this starting location. The estimated binding energy for this interaction for verapamil was −6.2 kcal/mol compared to −7.4 kcal/mol for daunorubicin at this site. Results of the six simulations we performed with verapamil starting at the preferred daunorubicin site were mixed. While an average movement of 4.5 Å toward the extracellular space was observed (Figure 4 of the Supporting Information), unlike with daunorubicin, two of the simulations showed <3 Å movement through the membrane and one simulation showed verapamil moving 4 Å from the extracellular space. The three other simulations showed movement of verapamil that was comparable to that observed when it started from its preferred docking position, moving between 7 and 11 Å toward the extracellular space (Figure 4 of the Supporting Information).

Overall, these latter experiments with daunorubicin or verapamil placed in nonoptimal positions within P-gp demonstrated that both of the transport substrates could be moved toward the extracellular space during the TMD-simulated catalytic cycles.

Movement of a Pyrophosphate Methyl Ester Out of the Drug Binding Sites of P-Glycoprotein and into the Cytoplasm. To test whether transport would be observed with a compound that clearly does not have the attributes of a good P-gp transport substrate, we placed a negatively charged, hydrophilic substance (pyrophosphate methyl ester) at the initial starting position of verapamil and performed simulations as described above. In these simulations, an entirely different behavior was observed when P-gp underwent the transition through the catalytic conformational changes. Pyrophosphate methyl ester does not fall into the category of compounds normally transported by P-gp, which are mostly hydrophobic molecules or hydrophobic cations.[3] Figure 3A (◆) shows the average position of methylpyrophosphate in six independent TMD simulations as P-gp moved from open to the inside to open to the outside conformation. As shown in Figure 3A, methylpyrophosphate immediately moved away from the drug binding sites of P-glycoprotein and away from the hydrophobic core of the phospholipid bilayer toward the cytoplasm during the simulations. A total of six such simulations were calculated for methylpyrophosphate, and each simulation (Figure 3D) showed this immediate movement of the polyanion into the cytoplasmic space.

Movement of Tariquidar, a P-Glycoprotein Inhibitor, during a Simulated Transport Cycle. In further experiments aimed at elucidating important ligand interactions that may occur during simulated transport cycles, we investigated a known inhibitor of P-glycoprotein, tariquidar.[42] In three different docking studies using tariquidar, we identified three separately located sites on P-gp that had high estimated ligand binding energies as calculated by AutoDock Vina (Figure 4). The highest-affinity tariquidar docking site (site 1 of Figure 4) was found using all of P-gp except the nucleotide binding domains as a docking target. The best docked example (from 300 replicates) had an estimated binding energy of −10.1 kcal/mol and was located in the intracellular loop (ICL) regions on TM4 and TM9 (see Table 2 of the Supporting Information for residues). For comparison, daunorubicin and verapamil docking at preferred sites within the drug binding domains had estimated binding energies of −7.6 and 7.4 kcal/mol, respectively. A second docking experiment targeted tariquidar to the entire drug binding domain but did not include the ICL regions of P-gp. The best example from this experiment (also 300 replicates) is shown in Figure 4 as site 2. This site was located at the level of the cytoplasmic leaflet in the drug binding sites and had an estimated binding energy of −9.1 kcal/mol. To also explore the drug binding site described in ref 71, a docking experiment was initiated that limited interactions to this area of the P-gp drug binding domain. These experiments resulted in the docking of tariquidar with an estimated affinity of −8.4 kcal/mol (site 3 in Figure 4).

The results of TMD simulations of transport cycles with these three tariquidar starting positions are presented in Figure 4. Figure 4B shows the average movement of the center of mass of tariquidar for all six replicates with one standard error of the mean represented by the error bars. Figure 4B (■) shows the movement of tariquidar when starting at the preferred docking site 1. Very little movement of tariquidar toward the extracellular space was observed from this starting position (~3.8 Å). It is also important to note that tariquidar bound at site 1 did not leave the region of P-gp with which it initially interacted in the docking experiments, and that it did not leave the ICL regions of P-gp. Importantly, residues D177 and N820 were observed to interact with tariquidar when the NBDs were in the closed positions in these simulations. These two residues were previously shown experimentally by Loo and Clarke[72] to activate ATP hydrolysis 10-fold when cross-linked as cysteine mutations. Stabilization of the close interaction of NBDs (and residues D177 and N820) by tariquidar may be important in its mechanism of inhibition (see Discussion).

When simulated transport cycles began with tariquidar at either site 2 or site 3 (both within the transmembrane drug binding sites of P-gp), much greater movement through the membrane toward the extracellular space was observed [averages of ~8 and ~10 Å from site 2 and site 3, respectively

DOI: 10.1021/acs.biochem.5b00018
Biochemistry 2015, 54, 4374−4390

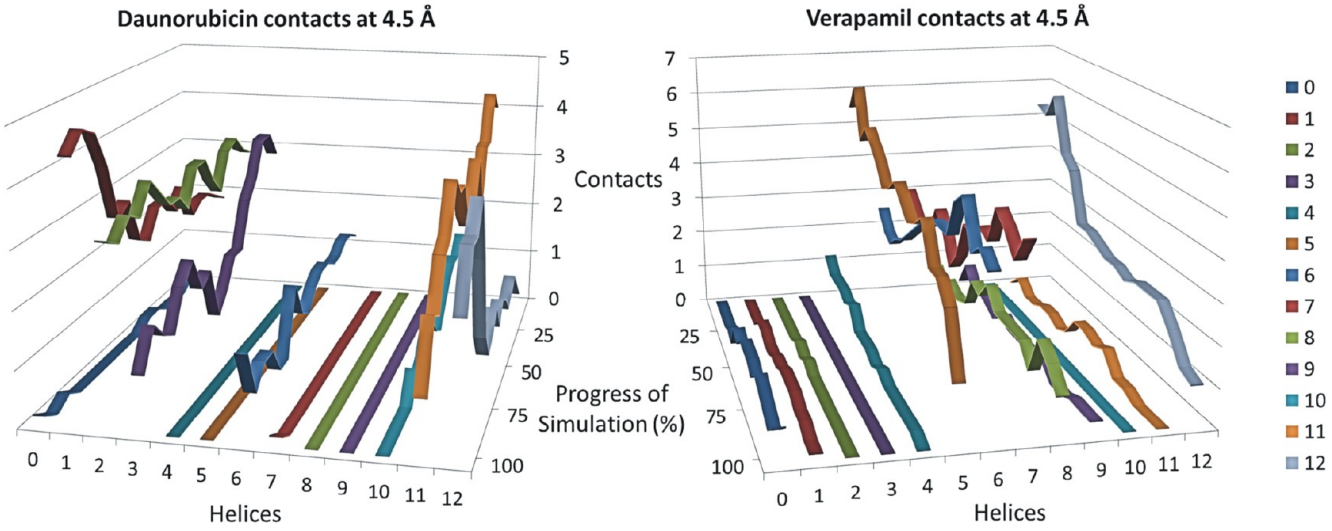

Figure 5. Average number of contacts made by transmembrane helices of P-glycoprotein during drug transport. The numbers of interactions of transport substrate with each of the 12 transmembrane helices of P-gp (helices 1−12, labeled on the *X*-axes) are plotted vs the progress of the simulations as P-gp cycled from the open to the inside conformations (0% on the "progress of simulation" *Y*-axes) to fully opened to the exterior conformations (100% on the *Y*-axes). Helix "0" represents any contact between protein and drug that occurred outside of the 12 transmembrane helices. The *Z*-axes show the number of contacts made at the various points in the simulation that were within 4.5 Å of any atom of P-gp. The color coding legend for the helices is shown on the right. The contact values were compiled for each of the six independently replicated simulations for each drug and then averaged. Results for daunorubicin transport are shown in the left panel while those for verapamil in the right panel.

(see Figure 4)]. These results suggest that tariquidar may be transported through the membrane by P-gp, if it is initially bound at a drug binding site within the transmembrane domain.

Two Transport Substrate Pathways through P-gp. Figure 5 shows the average number of contacts made by the individual transmembrane helices of P-gp (1−12) with either daunorubicin or verapamil over the course of the replicated simulations. These admittedly complex graphs show that very different patterns of contacts with the transmembrane helices of P-gp were observed for daunorubicin as compared with verapamil. During the transport of daunorubicin from its preferred docking position (Figure 5, left), TMs 1−3, 11, and 12 showed multiple contacts with the transport substrate over the course of the simulations, while TMs 6 and 10 had one or fewer contacts with the drug. Helices 4 and 7−9 did not interact at all with daunorubicin. For the transport of verapamil from its preferred starting position, a different pattern emerged (Figure 5, right). TMs 5−7 and 12 appeared to be very important in moving verapamil through the membrane, while TMs 4, 8, 9, and 11 interacted to an only minor extent. Helices 1−3 and 10 showed no interactions with verapamil over the course of the simulations. Neither daunorubicin nor verapamil significantly interacted with any residues outside of the transmembrane helices (designated as "helix 0" in the figure). Essentially the same results were obtained when 3.5 or 2.5 Å cutoff distances were chosen for these analyses (data not shown). These differences in which particular helices were used to drive either daunorubicin or verapamil through the membrane (as shown in Figure 5) appeared to be predetermined by the position in the protein in which the drug bound when the simulated transport cycles began. When daunorubicin was bound initially in its preferred binding site, TMs 1−3, 6, 11, and 12 were involved in its transport. When verapamil was initially bound in its preferred drug binding site, TMs 5−8 and 12 were involved in its transport. Both sets of simulations had in common only the "last" TMs of the half-transporter subunits, helices 6 and 12. These results suggest that there are at least two pathways through P-gp for transported substrates that are predetermined by which of the drug binding subsites is initially occupied by drug.

Stochastic Drug Contacts with Transmembrane Helices in the Two Transport Pathways through P-gp. Figures 6 and 7 and Figures 5 and 6 of the Supporting Information show that there is considerable variability when a particular transmembrane helix interacts with a drug and even which particular TM makes contact with a drug within either of these two pathways. As an example, Figures 5 and 6 of the Supporting Information show the contacts made between P-gp and daunorubicin and between P-gp and verapamil, respectively, in each of the six individual simulations. It is apparent that in the six individual simulations different TMs (1−3, 6, 11, and 12) were involved to differing extents in contacts that presumably pushed daunorubicin through the membrane portion of P-gp (Figure 5 of the Supporting Information). Very similar results indicating a large variability when different TMs interacted with verapamil were obtained when the six individual simulations of verapamil were plotted (Figure 6 of the Supporting Information). In the case of verapamil, TMs 5−8 and 12 were always involved, but some helices were contacted more often in some of the simulations than in others.

The observations that different helices seemed to dominate the interactions in some of the simulations while others dominated in other simulations are easier to visualize when the residuals of contacts relative to the average number of contacts between drug and TMs are plotted versus the progress of individual simulations (Figures 6 and 7 for daunorubicin and verapamil, respectively). The graphs show the differences between individual simulation runs and the averages of all simulations for each of the drugs. Large differences in contacts with any given transmembrane helix indicate that those helices are being used to different extents in the given simulations compared to average interactions. For example, in the daunorubicin simulations (Figure 6), TM helix 2 (green bars)

DOI: 10.1021/acs.biochem.5b00018
Biochemistry 2015, 54, 4374−4390

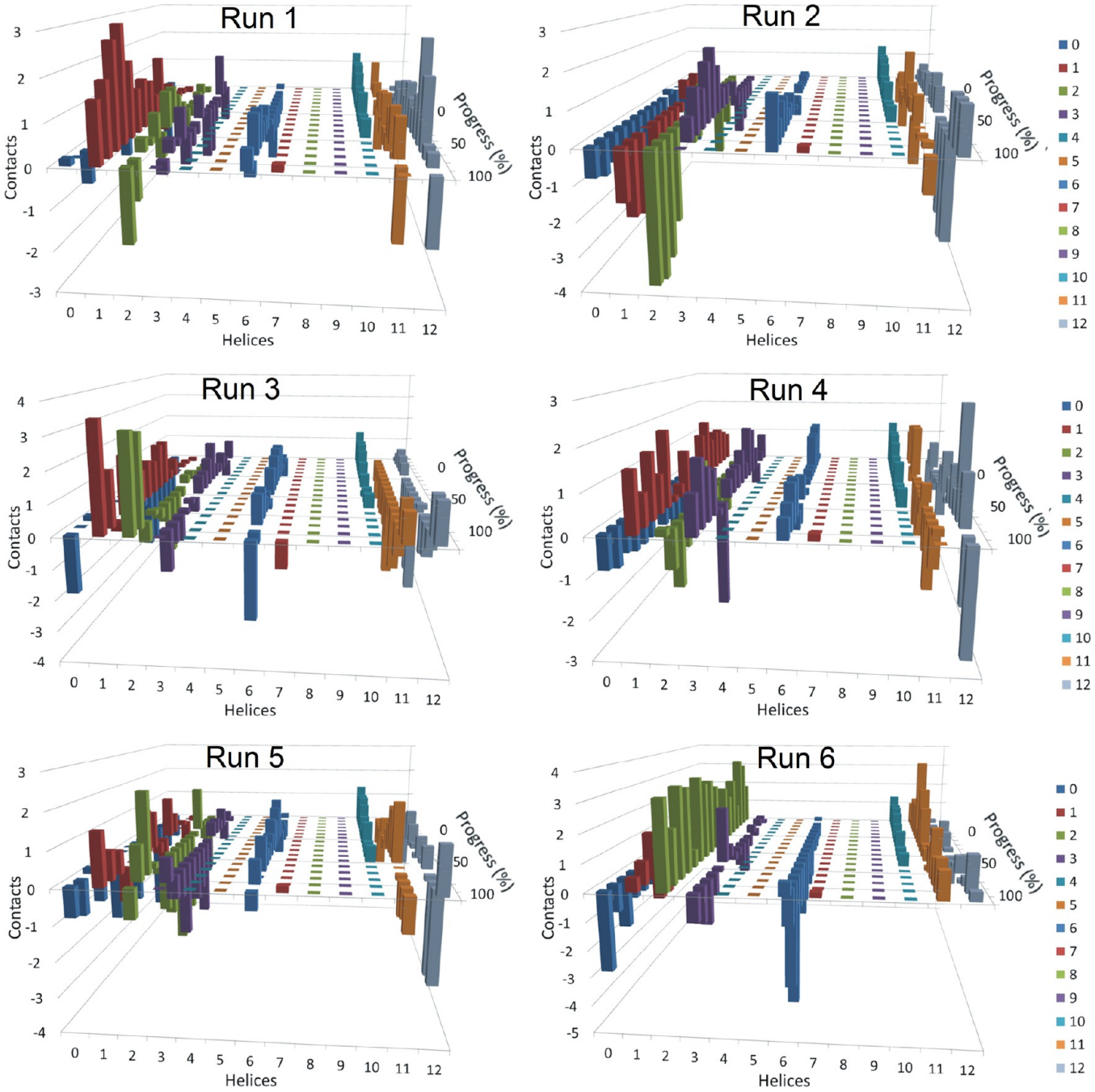

Figure 6. Residuals of the average numbers of contacts made by transmembrane helices of P-glycoprotein with daunorubicin for each independent simulation. These graphs are similar to those presented in Figure 5, except that the number of contacts at each point of progression in the six individual simulations with daunorubicin was subtracted from the average number of contacts at that point in the simulations. The graphs are intended to highlight the variability of contacts made between each transmembrane helix with daunorubicin as P-gp moved from open inside to open outside conformations. Results from six independent simulations are shown.

was used much more extensively in simulation 2 than in simulation 6. Conversely, TM helix 1 was used much less in simulation 1 than in simulation 2. Also, simulations 4 and 6 show very different patterns of daunorubicin contacts with helix 6 (blue). Other differences between individual simulations are also apparent from Figure 6.

Results of residual analyses between the average contacts of each TM and those observed in an individual verapamil transport simulation (Figure 7) led to comparable observations, even though different pathways and associated TM helices were involved. In the verapamil simulations, the effects seem to be even more dramatic than for the daunorubicin simulations. For example, comparison of the very different contacts of verapamil with helix 12 (light blue) in simulation 1, 2, 4, or 5 with those in simulation 3 or 6 highlights significant differences in the use and timing of the use of this helix in moving verapamil through P-gp. Likewise, contacts of TM 5 with verapamil (gold) were drastically different in simulation 2 compared with those in simulation 3 or 6. TM 7 also showed dramatically different contacts with verapamil in simulation 5 when compared to those in simulation 6. As a further example of the stochastic nature of the contacts of TMs with verapamil, TM 8 appeared

DOI: 10.1021/acs.biochem.5b00018
Biochemistry 2015, 54, 4374−4390

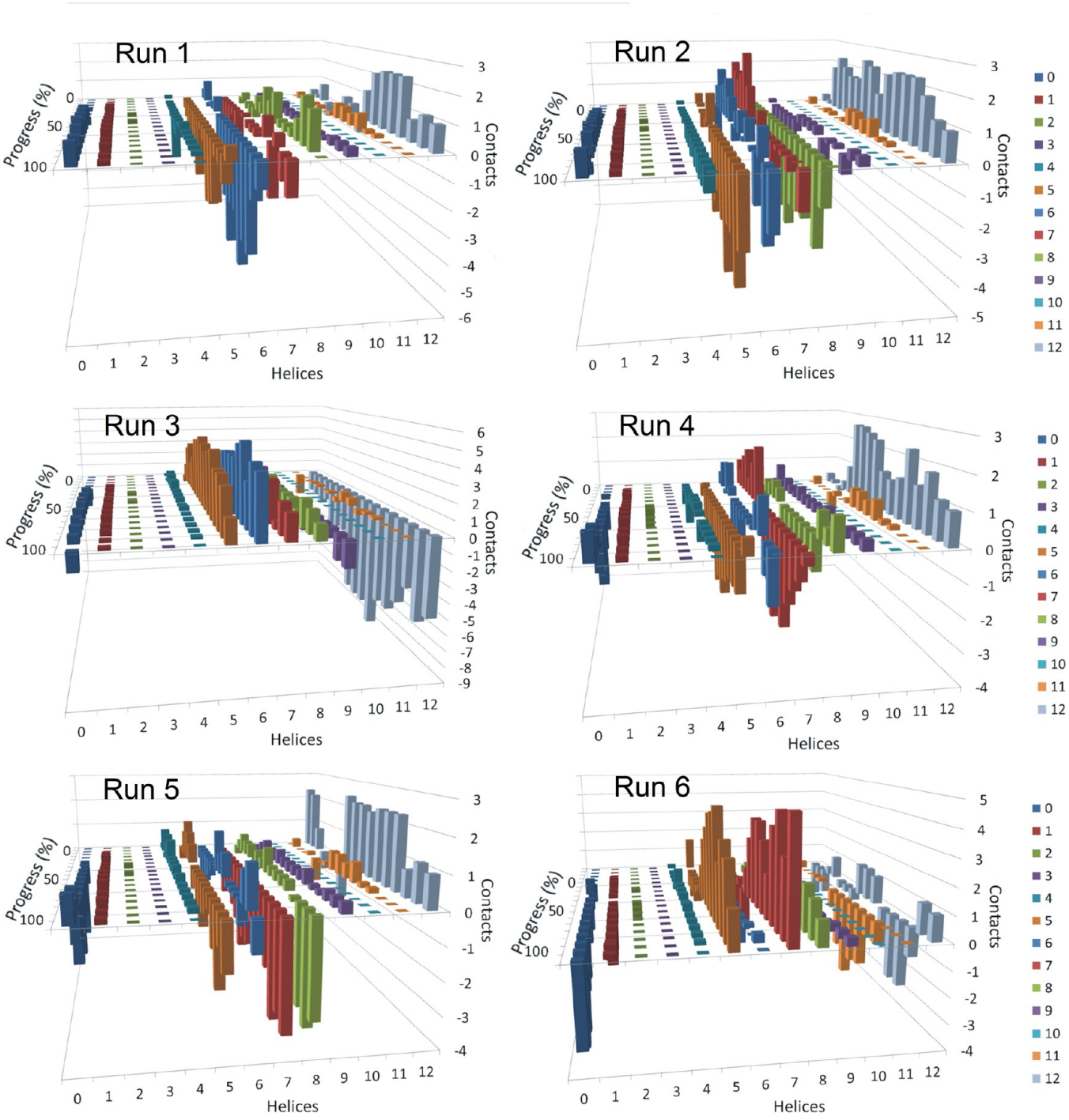

Figure 7. Residuals of the average number of contacts made by transmembrane helices of P-glycoprotein with verapamil for each independent simulation. These graphs are similar to those presented in Figure 5, except that the number of contacts at each point of progression in the six individual simulations with verapamil has been subtracted from the average number of contacts at that point in each of the six independent simulations.

to be heavily involved in drug interactions in simulation 2, but not in simulation 1, 3, or 6. These observations suggest that there is no predefined or predetermined step-by-step sequence of contacts for either of the two pathways for drugs through P-gp.

Nonpolar and Aromatic Interactions of P-Glycoprotein with Daunorubicin and Verapamil Dominate during Transport. Figure 8 presents the average number of contacts between transported drug and amino acids of each transmembrane helix for either daunorubicin (left panels) or verapamil (right panels) categorized for nonpolar amino acids (top panels), aromatic amino acids (middle panels), or polar residues (bottom panels). In the case of daunorubicin, nonpolar interactions in TMs 1, 2, and 12 appeared to be most important with minor interactions at TMs 3, 6, and 11. It appeared that aromatic interactions of daunorubicin with TM 11 were especially important when the protein was open to the cytoplasm and that the number these interactions decreased

DOI: 10.1021/acs.biochem.5b00018
Biochemistry 2015, 54, 4374−4390

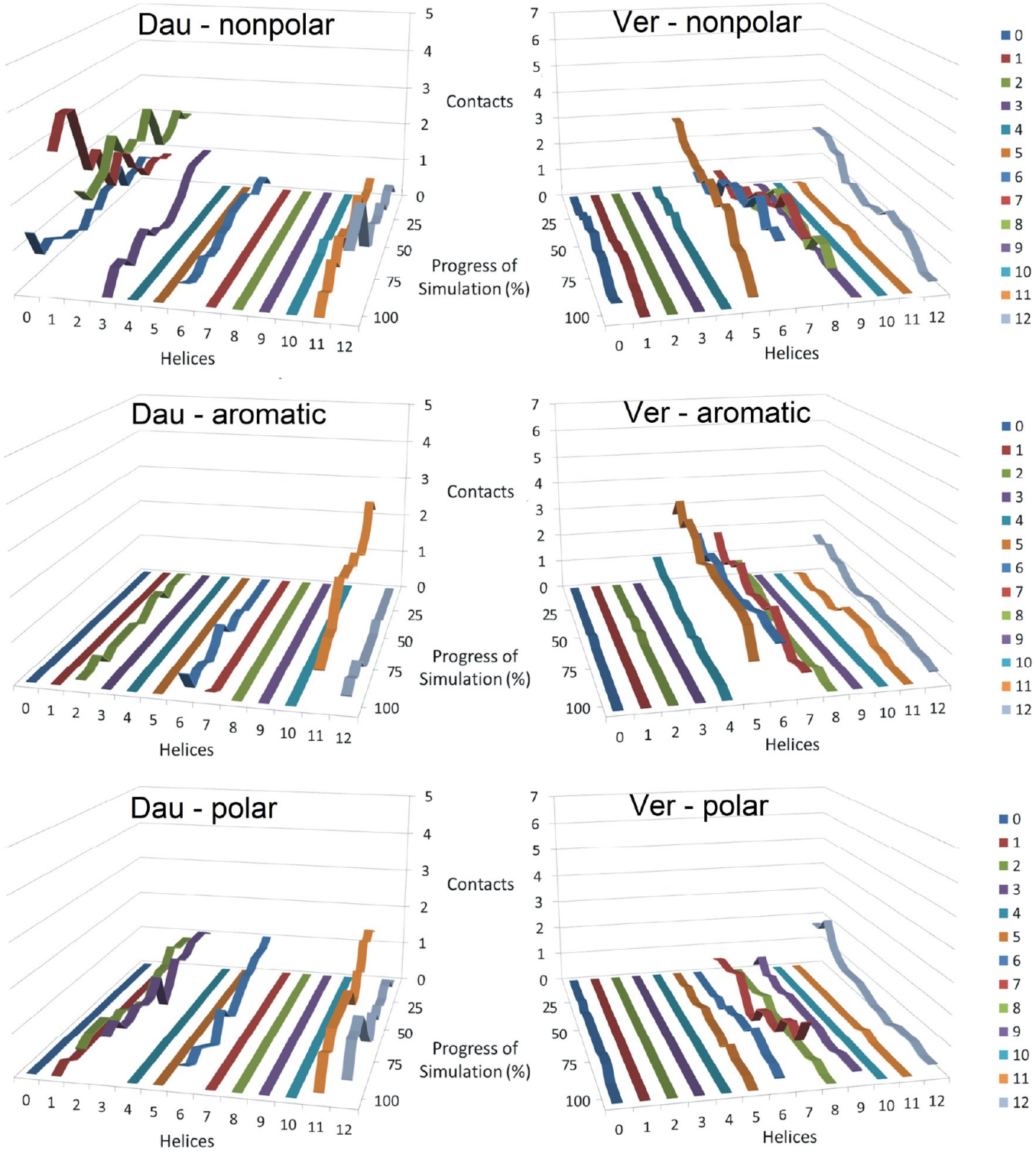

Figure 8. Interactions between P-gp and daunorubicin or verapamil with nonpolar, aromatic, or polar residues of the transmembrane helices. The figure presents the average number of contacts in all six replicate simulations for daunorubicin (left panels, "Dau") and verapamil (right panels, "Ver") for nonpolar (top), aromatic (middle), or polar (bottom) amino acid residues of P-gp. Graphs are plotted as described in the legend of Figure 5.

as P-gp progressed to open to the outside conformations. Verapamil showed both nonpolar and aromatic interactions with residues in TMs 5−7 and 12. Several interactions of both drugs with polar amino acids in the TM regions of P-gp were observed as is expected for these drugs, because both verapamil and daunorubicin have significant numbers of polar functional groups (6 polar groups in verapamil and 11 in daunorubicin). Figure 7 of the Supporting Information shows the results of similar analyses for contacts made between daunorubicin and verapamil with charged amino acid residues of the transmembrane helices of P-gp. Only the more polar daunorubicin was observed to interact with any charged residues (H61, K189,

DOI: 10.1021/acs.biochem.5b00018
Biochemistry 2015, 54, 4374−4390

D188, and E875). These interactions were minor, with fewer than one such charged residue interaction observed at any given stage of a simulation. No interactions with charged residues were observed for verapamil.

DISCUSSION

Binding Subsites for Daunorubicin and Verapamil on P-Glycoprotein. Ligand docking experiments were performed to position the transport substrates, daunorubicin and verapamil, into reasonable positions to analyze potential transport through P-glycoprotein in simulated catalytic cycles. These docking experiments resulted in preferred binding of daunorubicin and verapamil to two different subsites within the drug binding domain of P-gp in an open to the cytoplasm conformation (Figures 1 and 2 and Table 1 of the Supporting Information). Both drugs bound within the cytoplasmic leaflet part of the cell membrane. Daunorubicin preferentially bound to residues on TMs 1−3, 6, and 11, while verapamil docked preferentially to residues on TMs 4−8 and 12. Similar observations of different subsites on P-glycoprotein for drug binding have been previously reported.[25,26,31,38,73−78] It is interesting to point out that earlier work[73] suggested the presence of two distinct drug binding sites on P-gp that had different affinities for rhodamine 123 and Hoechst 33342, designated the R and H sites, respectively, and that the R site preferentially bound daunorubicin. In even earlier work,[60] it was observed that daunorubicin at low concentrations non-competitively inhibited verapamil transport but at high concentrations it competitively inhibited verapamil transport. As summarized in ref 73, these observations were taken to mean that daunorubicin and verapamil preferentially bound to different sites with daunorubicin binding at low concentrations at the R site and with verapamil at the H site. At high concentrations, daunorubicin appeared also to bind at the H site, competitively inhibiting verapamil transport.[73] It is tempting to think that the data for the docking of daunorubicin and verapamil to P-gp support these interpretations, because daunorubicin was observed to dock at two of the sites (preferring one site over the other) while verapamil preferentially bound to only one site and had to be forced into docking at the preferred daunorubicin site (the R site). The transport of verapamil from this latter starting point was also observed to be less consistent than when it started in its preferred position. Unfortunately, the accuracy of estimating binding energies using currently available docking software does not allow us to make this assertion with confidence.

It should be noted that both daunorubicin and verapamil were docked to P-gp under identical conditions. After the initial docking, the complete systems, including P-gp, drug, lipid, water, salt, nucleotide, and magnesium ion, were heated to 310 K and then equilibrated using molecular dynamics techniques (see Materials and Methods). These procedures allowed the docked drugs to independently readjust in each of the replicated simulations. This relaxation step varied the starting position of verapamil and daunorubicin somewhat before the targeted molecular dynamics was initiated. Quantification of this variation showed rmsd values relative to the initial docking position of 3.2 ± 0.4 Å with a range of 2.6−3.8 Å for daunorubicin and 4.9 ± 1.0 Å with a range of 3.9−6.7 Å for verapamil. Although a variety of protein−drug interactions were observed within each of the two subsites after equilibration, nonpolar and aromatic interactions clearly dominated for both daunorubicin and verapamil. The presence of many nonpolar and aromatic residues in these subsites (Figure 2 and Table 1 of the Supporting Information) may help explain some of the broad transport substrate specificities shown by P-gp, because these types of interactions would be available for many different hydrophobic or aromatic compounds. Interactions of polar residues with the somewhat more polar daunorubicin were more common than with the more hydrophobic verapamil. Only daunorubicin showed interactions with acidic and basic residues (Table 1 and Figure 7 of the Supporting Information). Daunorubicin also showed a few interactions outside of the transmembrane helices as defined in Uniprot (http://www.uniprot.org/uniprot/P08183), but these residues were all within approximately one helical turn of TM 10 and were in the lipid headgroup region of the cytoplasmic leaflet of the membrane.

The variable interactions of identically docked daunorubicin or verapamil to P-glycoprotein after molecular dynamics "incubation" at 310 K highlight the flexibility and plasticity of transport substrate binding to P-gp as mentioned by us previously.[31] The results also support and extend the hypothesis first introduced and tested by Loo and Clarke[79] that binding of the transport substrate to P-gp can induce conformational changes in the transmembrane helices that allow the binding of many different transport substrates. This induced fit model for P-gp[79] is extended here to two different subsites that have the flexibility to readjust binding in a dynamic way. These smaller adjustments of protein to ligand are shown here in the different contacts made between identically docked daunorubicin or verapamil after 310 K equilibrations (Table 1 of the Supporting Information).

Vectorial Transport of Verapamil and Daunorubicin through the Membrane by P-Glycoprotein. The studies presented here extend our previous work on the dynamic conformational changes that take place in the drug binding domains of P-gp during a putative catalytic cycle as simulated using targeted molecular dynamics techniques.[31] It should be reiterated here that these studies used four different targeted P-gp structures that were based on four crystal structures of related ABC transporters. The targeted molecular dynamics technique was used to push P-gp from one structure to the next. A limitation of TMD with only one target structure is that the method is blind to the nuances of movement of the protein in intermediate phases. Here we have employed multiple target structures that comprise intermediates that make biochemical and mechanistic sense. Although we cannot be certain that the lowest-energy path between these structures was sampled by the technique, what we can be sure of is that the targets used are close to low-energy conformations, because all four were derived from crystallized proteins. This study strongly suggests and reproducibly shows that the catalytic transport cycle simulated in these TMD experiments resulted in the net vectorial movement of two different transport ligands from binding positions within the cytoplasmic side of the membrane of P-gp to positions equivalent to the exterior leaflet of the membrane bilayer (summarized in Figure 3). During these simulations, the only external forces exerted on the system were directed at the protein, so any net movement from the cytoplasmic to the external side of the membrane must have been a consequence of the drug interacting with the protein. In other words, the vectorial movement of the transport substrates through the membrane was solely caused by the movement of P-gp transmembrane helices and the respective amino acid side chains that contacted the substrate. The movements of

DOI: 10.1021/acs.biochem.5b00018
Biochemistry 2015, 54, 4374−4390

transport substrates were from positions in P-glycoprotein equivalent to the cytoplasmic leaflet of the membrane bilayer at the start of the simulations to positions equivalent to the external side of the membrane (see Figures 1 and 3 and Figures 2−4 of the Supporting Information). The average movement of the calculated centers of mass of both drugs was 11−12 Å when starting at the preferred docking positions (see Figure 3). Daunorubicin when placed in the preferred verapamil docking site moved on average a similar distance toward the outside, while verapamil at its nonpreferred site moved less well on average but was observed in half of the simulations to move between 7 and 11 Å outward (Figure 4 of the Supporting Information). These results support the hypothesis that P-gp actually drives the drugs from one side of the membrane to the other. The results shown in Figure 3 and Figure 4 of the Supporting Information can be compared to those in Figure 8 of the Supporting Information that shows the results of net drug transport in terms of rmsd changes from the initial drug position to its final state at the end of the simulations.

A report using TMD techniques that were similar to those reported earlier by us[31] was recently published.[38] Despite using techniques and protein target structures similar to those reported here, the authors showed only very small rmsd changes of 1−2.5 Å for a series of P-gp transport substrates,[38] nearly 10-fold less than is presented here. One problem with rmsd measurements when using them to try to show vectorial movements as done in ref 38 is that a rotation of the molecule about its center of mass will show a large rmsd value when in fact the center of mass does not move. For this reason, we have preferred to use center of mass movement measurements instead of rmsd. However, to compare our results with those described in ref 38, we also calculated transport substrate rmsds. The maximal rmsd changes for simulations using daunorubicin and verapamil transport were 15.5 and 22.8 Å, respectively (see Figure 8 of the Supporting Information). These values were significantly larger than those reported in ref 38. The changes in rmsd reported in ref 38 may reflect slight movements and changes in conformation of compounds bound to essentially the same subsite on P-gp and the fact that no net vectorial movement of substrates was observed. One important interpretation of the simulations in ref 38 was that molecules thought to be inhibitors of transport by P-gp remained associated with residues in the initial docking sites longer than did molecules they listed as transport substrates. Because neither transport substrates nor inhibitors were shown in ref 38 to significantly move from the initial docking positions, this interpretation should be reevaluated.

In a manner independent of how we measured the transport of daunorubicin or verapamil (either by movement of the center of mass of the drug on the *Z*-axes as in Figure 3 or by rmsd as in Figure 8 of the Supporting Information), all 12 simulations reported here for the ligands bound to preferred docking sites demonstrated very significant movement of either daunorubicin or verapamil. Daunorubicin moved in six replicated simulations between 6 and 14 Å by center of mass on the *Z*-axes or up to 15.5 Å when measured by rmsd changes. Verapamil moved in six replicates by 8−20 Å transport by center of mass on the *Z*-axes or by up to 22.8 Å by rmsd changes.

Significantly, when we observed the movement of a polyanion, methylpyrophosphate, a compound that should not be transported by P-glycoprotein, no vectorial movement from inside to outside was observed (Figure 3A,D). In these simulations, where the methylpyrophosphate was placed directly into a drug binding site that we showed here was competent for verapamil transport, a movement in the direction opposite to that of verapamil or daunorubicin was observed (Figure 3A). Methylpyrophosphate moved quickly out of the verapamil drug binding subsite and toward the cytoplasmic space, while both verapamil and daunorubicin moved through the transmembrane domain of P-gp toward the extracellular space. In each of six replicated simulations, methylpyrophosphate moved 12−18 Å toward the cytoplasm.

These results with methylpyrophosphate are in stark contrast to the movement of either verapamil or daunorubicin during identical targeted molecular dynamics simulations. It should be emphasized that the methylpyrophosphate molecule was not docked in the verapamil subsite of drug binding sites of P-gp but was manually placed there to test whether an obvious nontransport substrate would also be driven through the membrane as P-gp underwent the transition from inside open to outside open conformations. The results presented in Figure 3 clearly show that a substance not meeting the criteria of a transport substrate of P-gp was not moved through the membrane by the protein but instead quickly moved toward the cytosol even when it was inserted into a drug binding site at the start of the simulation. This suggests that not just any substance that can be internalized into a drug binding site of P-gp will be actively transported. These simulations with methylpyrophosphate strongly support the hypothesis that the drug transport observed here with the known P-gp substrates daunorubicin and verapamil as the transporter cycled through a simulated catalytic cycle reflects a real drug transport mechanism of P-glycoprotein.

From the extent of the movements of daunorubicin and verapamil presented in Figure 3, it is clear that not just a repositioning of helices of P-gp has occurred that granted the drugs access to the outside of the membrane but that both daunorubicin and verapamil have been driven through the membrane toward the outside of the cell by the conformational changes that occurred during these catalytic cycles. The data strongly suggest that P-glycoprotein possesses a drug pumping activity and not just a differential gating activity that grants access of a drug from one membrane leaflet to the other.

Mechanism of Inhibition of P-Glycoprotein Transport by Tariquidar. Docking of tariquidar to P-glycoprotein in the open to the cytoplasm conformation was performed using three different targeting boxes for the ligand. In the first experiment, tariquidar was allowed to dock to any part of P-gp except the NBD structures, and this attempt found the docking position with the highest estimated affinity (−10.1 kcal/mol) of the three experiments (site 1 in Figure 4). This site was located in the intracellular loop (ICL) regions on TM4 and TM9. Tariquidar bound at this position was not transported through the membrane during transport cycle simulations (Figure 4) and was not observed to separate from the majority of the residues in its initial starting position.

It is relevant to the following that the initial starting interactions for tariquidar at site 1 included residues around N820 and that these residues stayed in the proximity of tariquidar throughout the entire simulation. In the latter part of these TMD simulations, when the NBDs were in a closed conformation thought to be competent for ATP binding and hydrolysis, tariquidar was also found to interact with residue D177. These two residues, D177 and N820, when mutated to cysteines and cross-linked, activated rates of ATP hydrolysis by

DOI: 10.1021/acs.biochem.5b00018
Biochemistry 2015, 54, 4374−4390

P-gp ~10-fold.[72] It is interesting to speculate that if tariquidar binds to site 1 and stabilizes the closed conformation of the NBDs, then this could explain the observations that tariquidar activates ATP hydrolysis by P-gp in the absence of transport.[72,80] This would also be consistent with tariquidar inhibiting transitions of P-gp to open conformations as determined in ref 81 in work that showed tariquidar inhibited the cross-linking of extracellularly located residues. Finally, if tariquidar binding at site 1 did stabilize conformations of P-gp with closed NBDs, it might also explain the tariquidar-dependent inhibition of the labeling of residues in the drug binding sites as described in ref 71. It should also be noted that tariquidar was observed to stabilize truncated drug binding domains of P-gp in ref 81 and that the residues reported here for tariquidar binding site 1 are present in these truncated P-gp peptides.

The fact that others observed inhibition of ATP hydrolysis by tariquidar[42] may perhaps be explained by tariquidar binding to P-gp at an alternative site or sites. When tariquidar was docked into the drug binding sites within P-gp (either site 2 or site 3 in Figure 4), significant transport of the inhibitor through the membrane and toward the extracellular space was observed (Figure 4). This suggested that tariquidar could be transported if it binds at drug binding sites on P-gp. Experimental data, however, suggest that tariquidar is not effectively transported by P-gp.[42,80] If tariquidar does bind to the drug binding sites of P-gp as implicated in ref 71, then one might speculate that tariquidar may not readily dissociate from P-gp even when it is exposed to the extracellular space at the end of a transport cycle, thereby inhibiting net turnover of the transporter and perhaps ATP hydrolysis. There is evidence that tariquidar binds significantly to the cell surface of P-gp-expressing cells,[80] and there is also strong evidence that tariquidar has a affinity for P-gp much higher than and an off-rate from P-gp slower than those of the good transport substrate, vinblastine.[42]

It is interesting to contrast these proposed mechanisms of inhibition by tariquidar to that proposed for other inhibitors of P-gp like the QZ59 peptides cocrystallized in murine P-gp structural studies.[26] In recent work, molecular dynamics studies of daunorubicin and the QZ59 inhibitors that suggest that inhibitors like QZ59-RRR and QZ59-SSS may inhibit P-gp by preventing NBD closure have been reported.[70]

Drug Transport through P-Glycoprotein Is both Predetermined and Stochastic. Figures 6 and 7 show clearly that the set of transmembrane helices involved in daunorubicin transport is different from that for verapamil transport through P-glycoprotein. Analyses of residues that contacted the different drugs as they were pushed through the transmembrane region of P-gp clearly showed that daunorubicin used TMs 1−3, 6, 11, and 12 while verapamil mainly used TMs 4−8, 11, and 12. Only TMs 6 and 12 (and to a minor extent 11) were common to both subsets, and both subsets correlated nearly perfectly with the initial binding subsets for the two substrates. This strongly suggests that the initial site of binding of a drug to P-gp may predetermine which P-gp substructures are involved in pushing the drug all the way through to the external side of the membrane. In this sense, it appears to be significant that the general path a drug takes through P-gp is predetermined by which initial subsite in the drug binding sites a given drug binds. This is an important conclusion about the structure and mechanism of drug transport through P-gp that can be inferred from Figure 5 and Table 1 of the Supporting Information.

A second important inference that can be made from this work is that within these two general pathways through P-gp, there does not appear to be a single defined path of contacts that drives a transport substrate out of the cell. Figures 6 and 7 (and Figures 5 and 6 of the Supporting Information) indicate that within each of the two observed pathways through P-gp, the contacts between TM helices and the drug as any given simulation progressed showed much variation in which TM interacted with a specific drug and even when specific TMs interacted with each drug. These observations suggest that stochastic opportunistic contacts between protein and transport substrate within each of the two general pathways drive the drug through the membrane. We observed that nonpolar and aromatic amino acids contacted transported drugs most often as they were pushed toward the external space by P-gp and that there were significantly more polar and charged amino acid contacts with the more polar daunorubicin than with verapamil.

Conclusions. The simulations of catalytic transport cycles by P-glycoprotein with different transport substrates presented in this study directly demonstrated that transport drugs can be actively pushed by the protein an average of 11−12 Å from the cytoplasmic to the external side of the membrane. At the same time, access of the transported drug was changed from inside membrane surfaces and cytoplasmic bulk phase solvent to outside membrane surfaces and external bulk solvent. The simulations suggested that there are two pathways for transport substrates through P-gp and that the starting location of the drugs, one of two different drug binding subsites, predetermined which pathway would be used. Additionally, the results suggested that the actual transmembrane helices involved in pushing the drugs through the membrane and the timing of the contacts between protein and drug in either of the two pathways could vary in what appeared to be a stochastic manner. The observations presented here elucidated several characteristics about the mechanism of drug transport through P-glycoprotein. (1) There are at least two different drug binding subsites in the transmembrane domains of P-gp that can preferentially bind transport substrates. (2) It appears that there are at least two different general pathways for a transport substrate to be pushed through the membrane, (3) that the general pathway used by a particular transport substrate appears to be correlated with its initial drug binding subsite, and (4) that within either of the two general pathways for a drug through P-gp, the actual contacts between TMs and drug and the timing of the contacts can be highly variable and stochastic in nature. In additional studies, the strong inhibitor of P-gp, tariquidar, was observed to dock at three plausible sites. The preferred site for tariquidar docking was in the intracellular loop region on TMs 4 and 9. Transport of tariquidar through the membrane from this site was not observed. Alternatively, positioning tariquidar within drug binding domains resulted in movement of tariquidar through the membrane. We speculate that in the former case, stabilization of NBD-closed conformations through tariquidar binding explains both the inhibition of transport and stimulation of ATP hydrolysis by P-gp that has been observed. Transport through the membrane in the latter case, coupled with slow dissociation of tariquidar, may inhibit both hydrolysis and transport by P-gp.

DOI: 10.1021/acs.biochem.5b00018
Biochemistry 2015, 54, 4374−4390

■ ASSOCIATED CONTENT

Supporting Information

Additional data and two movies. The Supporting Information is available free of charge on the ACS Publications website at DOI: 10.1021/acs.biochem.5b00018.

■ AUTHOR INFORMATION

Corresponding Author

*E-mail: jwise@smu.edu. Phone: 214-768-3426. Fax: 214-768-3955.

Funding

This project was supported by Grant 1R15GM094771-01A1 from the National Institute of General Medical Sciences to P.D.V. and J.G.W. and by the Communities Foundation of Texas, the SMU University Research Council, the SMU Dedman College Dean's Research Council, and the SMU Dedman College Center for Drug Discovery, Design and Delivery.

Notes

The authors declare no competing financial interest.

■ ACKNOWLEDGMENTS

Computational resources were provided by the SMU Center for Scientific Computing. A special thanks to Professor Junmei Wang (University of Texas Southwestern Medical Center) for helpful discussions and to Joe Gargiula and Amit Kumar of the SMU Office of Information Technology for their assistance with this work. We also thank the reviewers of the paper for their constructive suggestions.

■ ABBREVIATIONS

ABCB1, ATP binding cassette transporter, type B1; DBD, drug binding domain, the domain of the transporter consisting of the 12 transmembraneous helices and the intracellular extensions of these helices; ICL, intracellular loop region; MD, molecular dynamics; NBD, nucleotide binding domain; *NPT*, isothermic–isobaric molecular simulation ensemble in which the number of atoms, pressure, and temperature are held constant; P-gp, P-glycoprotein; POPC, 1-palmitoyl-2-oleoyl-*sn*-glycero-3-phosphocholine; rmsd, root-mean-square deviation; TM, transmembrane helix; TMD, targeted molecular dynamics.

■ REFERENCES

(1) Cascorbi, I. (2011) P-glycoprotein: tissue distribution, substrates, and functional consequences of genetic variations. *Handbook of experimental pharmacology*, 261–283.

(2) Eckford, P. D., and Sharom, F. J. (2009) ABC efflux pump-based resistance to chemotherapy drugs. *Chem. Rev. 109*, 2989–3011.

(3) Schinkel, A. H., and Jonker, J. W. (2003) Mammalian drug efflux transporters of the ATP binding cassette (ABC) family: an overview. *Adv. Drug Delivery Rev. 55*, 3–29.

(4) Cordon-Cardo, C., O'Brien, J. P., Boccia, J., Casals, D., Bertino, J. R., and Melamed, M. R. (1990) Expression of the multidrug resistance gene product (P-glycoprotein) in human normal and tumor tissues. *J. Histochem. Cytochem. 38*, 1277–1287.

(5) Lee, C. A., Cook, J. A., Reyner, E. L., and Smith, D. A. (2010) P-glycoprotein related drug interactions: clinical importance and a consideration of disease states. *Expert Opin. Drug Metab. Toxicol. 6*, 603–619.

(6) Juliano, R. L., and Ling, V. (1976) A surface glycoprotein modulating drug permeability in Chinese hamster ovary cell mutants. *Biochim. Biophys. Acta, Biomembr. 455*, 152–162.

(7) Shen, D. W., Fojo, A., Roninson, I. B., Chin, J. E., Soffir, R., Pastan, I., and Gottesman, M. M. (1986) Multidrug resistance of DNA-mediated transformants is linked to transfer of the human mdr1 gene. *Molecular and cellular biology 6*, 4039–4045.

(8) Marquez, B., and Van Bambeke, F. (2011) ABC multidrug transporters: target for modulation of drug pharmacokinetics and drug-drug interactions. *Current drug targets 12*, 600–620.

(9) Vogelgesang, S., Kuhnke, D., Jedlitschky, G., Jucker, M., Mosyagin, I., Pahnke, J., Cascorbi, I., Kroemer, H. K., Walker, L. C., and Warzok, R. W. (2006) P-glycoprotein (ABCB1) mediates transport of Alzheimer's beta-amyloid peptides. *Acta Neuropathol 112*, 365–367.

(10) Pahnke, J., Langer, O., and Krohn, M. (2014) Alzheimer's and ABC transporters - new opportunities for diagnostics and treatment. *Neurobiol. Dis. 72* (Part A), 54–60.

(11) Varatharajan, L., and Thomas, S. A. (2009) The transport of anti-HIV drugs across blood-CNS interfaces: summary of current knowledge and recommendations for further research. *Antiviral Res. 82*, A99–109.

(12) Chen, C. J., Chin, J. E., Ueda, K., Clark, D. P., Pastan, I., Gottesman, M. M., and Roninson, I. B. (1986) Internal duplication and homology with bacterial transport proteins in the mdr1 (P-glycoprotein) gene from multidrug-resistant human cells. *Cell 47*, 381–389.

(13) Senior, A. E. (1998) Catalytic mechanism of P-glycoprotein. *Acta Physiol Scand Suppl 643*, 213–218.

(14) Sauna, Z. E., Smith, M. M., Muller, M., Kerr, K. M., and Ambudkar, S. V. (2001) The mechanism of action of multidrug-resistance-linked P-glycoprotein. *J. Bioenerg. Biomembr. 33*, 481–491.

(15) Loo, T. W., Bartlett, M. C., and Clarke, D. M. (2003) Drug binding in human P-glycoprotein causes conformational changes in both nucleotide-binding domains. *J. Biol. Chem. 278*, 1575–1578.

(16) Sharom, F. J., Lugo, M. R., and Eckford, P. D. (2005) New insights into the drug binding, transport and lipid flippase activities of the p-glycoprotein multidrug transporter. *J. Bioenerg. Biomembr. 37*, 481–487.

(17) Sauna, Z. E., and Ambudkar, S. V. (2007) About a switch: how P-glycoprotein (ABCB1) harnesses the energy of ATP binding and hydrolysis to do mechanical work. *Mol. Cancer Ther. 6*, 13–23.

(18) Dawson, R. J. P., Hollenstein, K., and Locher, K. P. (2007) Uptake or extrusion: crystal structures of full ABC transporters suggest a common mechanism. *Mol. Microbiol. 65*, 250–257.

(19) Ward, A., Reyes, C. L., Yu, J., Roth, C. B., and Chang, G. (2007) Flexibility in the ABC transporter MsbA: Alternating access with a twist. *Proc. Natl. Acad. Sci. U. S. A. 104*, 19005–19010.

(20) Verhalen, B., Ernst, S., Borsch, M., and Wilkens, S. (2012) Dynamic ligand-induced conformational rearrangements in P-glycoprotein as probed by fluorescence resonance energy transfer spectroscopy. *J. Biol. Chem. 287*, 1112–1127.

(21) Verhalen, B., and Wilkens, S. (2011) P-glycoprotein retains drug-stimulated ATPase activity upon covalent linkage of the two nucleotide binding domains at their C-terminal ends. *J. Biol. Chem. 286*, 10476–10482.

(22) Dawson, R. J. P., and Locher, K. P. (2006) Structure of a bacterial multidrug ABC transporter. *Nature 443*, 180–185.

(23) Hollenstein, K., Dawson, R. J. P., and Locher, K. P. (2007) Structure and mechanism of ABC transporter proteins. *Curr. Opin. Struct. Biol. 17*, 412–418.

(24) Sauna, Z. E., Kim, I. W., and Ambudkar, S. V. (2007) Genomics and the mechanism of P-glycoprotein (ABCB1). *J. Bioenerg. Biomembr. 39*, 481–487.

(25) Ward, A. B., Szewczyk, P., Grimard, V., Lee, C. W., Martinez, L., Doshi, R., Caya, A., Villaluz, M., Pardon, E., Cregger, C., Swartz, D. J., Falson, P. G., Urbatsch, I. L., Govaerts, C., Steyaert, J., and Chang, G. (2013) Structures of P-glycoprotein reveal its conformational flexibility and an epitope on the nucleotide-binding domain. *Proc. Natl. Acad. Sci. U. S. A. 110*, 13386–13391.

(26) Li, J., Jaimes, K. F., and Aller, S. G. (2014) Refined structures of mouse P-glycoprotein. *Protein Sci. 23*, 34–46.

DOI: 10.1021/acs.biochem.5b00018
Biochemistry 2015, 54, 4374–4390

(27) Jin, M. S., Oldham, M. L., Zhang, Q., and Chen, J. (2012) Crystal structure of the multidrug transporter P-glycoprotein from Caenorhabditis elegans. *Nature 490*, 566−569.
(28) Wen, P. C., Verhalen, B., Wilkens, S., McHaourab, H. S., and Tajkhorshid, E. (2013) On the origin of large flexibility of P-glycoprotein in the inward-facing state. *J. Biol. Chem. 288*, 19211−19220.
(29) Dawson, R. J. P., and Locher, K. P. (2007) Structure of the multidrug ABC transporter Sav1866 from Staphylococcus aureus in complex with AMP-PNP. *FEBS Lett. 581*, 935−938.
(30) Velamakanni, S., Yao, Y., Gutmann, D. A. P., and van Veen, H. W. (2008) Multidrug transport by the ABC transporter Sav1866 from Staphylococcus aureus. *Biochemistry 47*, 9300−9308.
(31) Wise, J. G. (2012) Catalytic transitions in the human MDR1 P-glycoprotein drug binding sites. *Biochemistry 51*, 5125−5141.
(32) Amaro, R. E., Baron, R., and McCammon, J. A. (2008) An improved relaxed complex scheme for receptor flexibility in computer-aided drug design. *J. Comput.-Aided Mol. Des. 22*, 693−705.
(33) Ivetac, A., and McCammon, J. A. (2011) Molecular recognition in the case of flexible targets. *Curr. Pharm. Des 17*, 1663−1671.
(34) Lin, J.-H., Perryman, A. L., Schames, J. R., and McCammon, J. A. (2002) Computational drug design accommodating receptor flexibility: the relaxed complex scheme. *J. Am. Chem. Soc. 124*, 5632−5633.
(35) Roberts, E., Eargle, J., Wright, D., and Luthey-Schulten, Z. (2006) MultiSeq: unifying sequence and structure data for evolutionary analysis. *BMC Bioinf. 7*, 382.
(36) Aller, S. G., Yu, J., Ward, A., Weng, Y., Chittaboina, S., Zhuo, R., Harrell, P. M., Trinh, Y. T., Zhang, Q., Urbatsch, I. L., and Chang, G. (2009) Structure of P-glycoprotein reveals a molecular basis for poly-specific drug binding. *Science 323*, 1718−1722.
(37) Brewer, F. K., Follit, C. A., Vogel, P. D., and Wise, J. G. (2014) In silico Screening for Inhibitors of P-Glycoprotein that Target the Nucleotide Binding Domains. *Mol. Pharmacol. 86*, 716−726.
(38) Prajapati, R., and Sangamwar, A. T. (2014) Translocation mechanism of P-glycoprotein and conformational changes occurring at drug-binding site: Insights from multi-targeted molecular dynamics. *Biochim. Biophys. Acta, Biomembr. 1838*, 2882−2898.
(39) Tsuruo, T., Iida, H., Tsukagoshi, S., and Sakurai, Y. (1981) Overcoming of vincristine resistance in P388 leukemia in vivo and in vitro through enhanced cytotoxicity of vincristine and vinblastine by verapamil. *Cancer research 41*, 1967−1972.
(40) Rogan, A. M., Hamilton, T. C., Young, R. C., Klecker, R. W., Jr., and Ozols, R. F. (1984) Reversal of adriamycin resistance by verapamil in human ovarian cancer. *Science 224*, 994−996.
(41) Ozols, R. F., Cunnion, R. E., Klecker, R. W., Jr., Hamilton, T. C., Ostchega, Y., Parrillo, J. E., and Young, R. C. (1987) Verapamil and adriamycin in the treatment of drug-resistant ovarian cancer patients. *Journal of clinical oncology: official journal of the American Society of Clinical Oncology 5*, 641−647.
(42) Martin, C., Berridge, G., Mistry, P., Higgins, C., Charlton, P., and Callaghan, R. (1999) The molecular interaction of the high affinity reversal agent XR9576 with P-glycoprotein. *Br. J. Pharmacol. 128*, 403−411.
(43) Humphrey, W., Dalke, A., and Schulten, K. (1996) VMD: visual molecular dynamics. *J. Mol. Graphics 14*, 33−38.
(44) Phillips, J. C., Braun, R., Wang, W., Gumbart, J., Tajkhorshid, E., Villa, E., Chipot, C., Skeel, R. D., Kalé, L., and Schulten, K. (2005) Scalable molecular dynamics with NAMD. *J. Comput. Chem. 26*, 1781−1802.
(45) MacKerell, A., Jr, Bashford, D., Bellott, M., Dunbrack, R., Jr, Evanseck, J., Field, M., Fischer, S., Gao, J., Guo, H., Ha, S., Joseph-McCarthy, D., Kuchnir, L., Kuczera, K., Lau, F., Mattos, C., Michnick, S., Ngo, T., Nguyen, D., Prodhom, B., Reiher, W., III, Roux, B., Schlenkrich, M., Smith, J., Stote, R., Straub, J., Watanabe, M., Wiorkiewicz-Kuczera, J., Yin, D., and Karplus, M. (1998) All-atom empirical potential for molecular modeling and dynamics Studies of proteins. *J. Phys. Chem. B 102*, 3586−3616.
(46) Morris, G. M., Huey, R., Lindstrom, W., Sanner, M. F., Belew, R. K., Goodsell, D. S., and Olson, A. J. (2009) AutoDock4 and AutoDockTools4: Automated docking with selective receptor flexibility. *J. Comput. Chem. 30*, 2785−2791.
(47) Trott, O., and Olson, A. J. (2010) AutoDock Vina: improving the speed and accuracy of docking with a new scoring function, efficient optimization, and multithreading. *J. Comput. Chem. 31*, 455−461.
(48) Hornung, T., Volkov, O. A., Zaida, T. M., Delannoy, S., Wise, J. G., and Vogel, P. D. (2008) Structure of the cytosolic part of the subunit b-dimer of Escherichia coli F0F1-ATP synthase. *Biophys. J. 94*, 5053−5064.
(49) Schmidt, M. W., Baldridge, K. K., Boatz, J. A., Elbert, S. T., Gordon, M. S., Jensen, J. H., Koseki, S., Matsunaga, N., Nguyen, K. A., Su, S. J., Windus, T. L., Dupuis, M., and Montgomery, J. A. (1993) General Atomic and Molecular Electronic-Structure System. *J. Comput. Chem. 14*, 1347−1363.
(50) Sale, K., Sár, C., Sharp, K. A., Hideg, K., and Fajer, P. G. (2002) Structural determination of spin label immobilization and orientation: a Monte Carlo minimization approach. *J. Magn. Reson. 156*, 104−112.
(51) Wang, J., Wang, W., Kollman, P. A., and Case, D. A. (2006) Automatic atom type and bond type perception in molecular mechanical calculations. *J. Mol. Graphics Modell. 25*, 247−260.
(52) Case, D. A., Cheatham, T. E., 3rd, Darden, T., Gohlke, H., Luo, R., Merz, K. M., Jr., Onufriev, A., Simmerling, C., Wang, B., and Woods, R. J. (2005) The Amber biomolecular simulation programs. *J. Comput. Chem. 26*, 1668−1688.
(53) Wang, J., Wolf, R. M., Caldwell, J. W., Kollman, P. A., and Case, D. A. (2004) Development and testing of a general amber force field. *J. Comput. Chem. 25*, 1157−1174.
(54) Jakalian, A., Bush, B. L., Jack, D. B., and Bayly, C. I. (2000) Fast, efficient generation of high-quality atomic Charges. AM1-BCC model: I. Method. *J. Comput. Chem. 21*, 132−146.
(55) Jakalian, A., Jack, D. B., and Bayly, C. I. (2002) Fast, efficient generation of high-quality atomic charges. AM1-BCC model: II. Parameterization and validation. *J. Comput. Chem. 23*, 1623−1641.
(56) Engels, M., Jacoby, E., Krüger, P., Schlitter, J., and Wollmer, A. (1992) The T<−>R structural transition of insulin; pathways suggested by targeted energy minimization. *Protein Eng., Des. Sel. 5*, 669−677.
(57) Schlitter, J., Engels, M., and Krüger, P. (1994) Targeted molecular dynamics: a new approach for searching pathways of conformational transitions. *J. Mol. Graphics 12*, 84−89.
(58) Russell, R. B., and Barton, G. J. (1992) Multiple protein sequence alignment from tertiary structure comparison: assignment of global and residue confidence levels. *Proteins: Struct., Funct., Genet. 14*, 309−323.
(59) Eargle, J., Wright, D., and Luthey-Schulten, Z. (2006) Multiple Alignment of protein structures and sequences for VMD. *Bioinformatics 22*, 504−506.
(60) Spoelstra, E. C., Westerhoff, H. V., Pinedo, H. M., Dekker, H., and Lankelma, J. (1994) The multidrug-resistance-reverser verapamil interferes with cellular P-glycoprotein-mediated pumping of daunorubicin as a non-competing substrate. *Eur. J. Biochem. 221*, 363−373.
(61) Omote, H., and Al-Shawi, M. K. (2002) A novel electron paramagnetic resonance approach to determine the mechanism of drug transport by P-glycoprotein. *J. Biol. Chem. 277*, 45688−45694.
(62) Loo, T. W., and Clarke, D. M. (2005) Do drug substrates enter the common drug-binding pocket of P-glycoprotein through "gates"? *Biochem. Biophys. Res. Commun. 329*, 419−422.
(63) Loo, T. W., Bartlett, M. C., and Clarke, D. M. (2006) Transmembrane segment 7 of human P-glycoprotein forms part of the drug-binding pocket. *Biochem. J. 399*, 351−359.
(64) Loo, T. W., Bartlett, M. C., and Clarke, D. M. (2006) Transmembrane segment 1 of human P-glycoprotein contributes to the drug-binding pocket. *Biochem. J. 396*, 537−545.
(65) Loo, T. W., Bartlett, M. C., and Clarke, D. M. (2007) Suppressor mutations in the transmembrane segments of P-glycoprotein promote maturation of processing mutants and disrupt a subset of drug-binding sites. *J. Biol. Chem. 282*, 32043−32052.

DOI: 10.1021/acs.biochem.5b00018
Biochemistry 2015, 54, 4374−4390

(66) Loo, T. W., Bartlett, M. C., and Clarke, D. M. (2008) Arginines in the first transmembrane segment promote maturation of a P-glycoprotein processing mutant by hydrogen bond interactions with tyrosines in transmembrane segment 11. *J. Biol. Chem. 283*, 24860−24870.
(67) Loo, T. W., and Clarke, D. M. (2008) Mutational analysis of ABC proteins. *Arch. Biochem. Biophys. 476*, 51−64.
(68) Loo, T. W., Bartlett, M. C., and Clarke, D. M. (2009) Identification of residues in the drug translocation pathway of the human multidrug resistance P-glycoprotein by arginine mutagenesis. *J. Biol. Chem. 284*, 24074−24087.
(69) Loo, T. W., and Clarke, D. M. (2013) Drug rescue distinguishes between different structural models of human P-glycoprotein. *Biochemistry 52*, 7167−7169.
(70) Ma, J., and Biggin, P. C. (2013) Substrate versus inhibitor dynamics of P-glycoprotein. *Proteins: Struct., Funct., Genet. 81*, 1653−1668.
(71) Chufan, E. E., Kapoor, K., Sim, H. M., Singh, S., Talele, T. T., Durell, S. R., and Ambudkar, S. V. (2013) Multiple transport-active binding sites are available for a single substrate on human P-glycoprotein (ABCB1). *PLoS One 8*, e82463.
(72) Loo, T. W., Bartlett, M. C., Detty, M. R., and Clarke, D. M. (2012) The ATPase activity of the P-glycoprotein drug pump is highly activated when the N-terminal and central regions of the nucleotide-binding domains are linked closely together. *J. Biol. Chem. 287*, 26806−26816.
(73) Shapiro, A. B., and Ling, V. (1997) Positively cooperative sites for drug transport by P-glycoprotein with distinct drug specificities. *Eur. J. Biochem. 250*, 130−137.
(74) Loo, T. W., and Clarke, D. M. (2000) Identification of residues within the drug-binding domain of the human multidrug resistance P-glycoprotein by cysteine-scanning mutagenesis and reaction with dibromobimane. *J. Biol. Chem. 275*, 39272−39278.
(75) Loo, T. W., and Clarke, D. M. (1999) Identification of residues in the drug-binding domain of human P-glycoprotein. Analysis of transmembrane segment 11 by cysteine-scanning mutagenesis and inhibition by dibromobimane. *J. Biol. Chem. 274*, 35388−35392.
(76) Loo, T. W., and Clarke, D. M. (1997) Identification of residues in the drug-binding site of human P-glycoprotein using a thiol-reactive substrate. *J. Biol. Chem. 272*, 31945−31948.
(77) Loo, T. W., and Clarke, D. M. (2002) Location of the rhodamine-binding site in the human multidrug resistance P-glycoprotein. *J. Biol. Chem. 277*, 44332−44338.
(78) Loo, T. W., Bartlett, M. C., and Clarke, D. M. (2003) Simultaneous binding of two different drugs in the binding pocket of the human multidrug resistance P-glycoprotein. *J. Biol. Chem. 278*, 39706−39710.
(79) Loo, T. W., Bartlett, M. C., and Clarke, D. M. (2003) Substrate-induced conformational changes in the transmembrane segments of human P-glycoprotein. Direct evidence for the substrate-induced fit mechanism for drug binding. *J. Biol. Chem. 278*, 13603−13606.
(80) Kannan, P., Telu, S., Shukla, S., Ambudkar, S. V., Pike, V. W., Halldin, C., Gottesman, M. M., Innis, R. B., and Hall, M. D. (2011) The "specific" P-glycoprotein inhibitor Tariquidar is also a substrate and an inhibitor for breast cancer resistance protein (BCRP/ABCG2). *ACS Chem. Neurosci. 2*, 82−89.
(81) Loo, T. W., and Clarke, D. M. (2014) Tariquidar inhibits P-glycoprotein drug efflux but activates ATPase activity by blocking transition to an open conformation. *Biochem. Pharmacol. 92*, 558−566.

DOI: 10.1021/acs.biochem.5b00018
Biochemistry 2015, 54, 4374−4390